Microscopic mechanisms of cooperative communications within single nanocatalysts

Bhawakshi Punia[a], Srabanti Chaudhury[a,1,2], and Anatoly B. Kolomeisky[b,c,d,e,1,2]

[a]Department of Chemistry, Indian Institute of Science Education and Research, Pune, 411008 India; [b]Department of Chemistry, Rice University, Houston, TX 77005-1892; [c]Center for Theoretical Biological Physics, Rice University, Houston, TX 77005-1892; [d]Department of Chemical and Biomolecular Engineering, Rice University, Houston, TX 77005-1892; and [e]Department of Physics and Astronomy, Rice University, Houston, TX 77005-1892

Edited by Thirumalai Devarajan, University of Texas at Austin, Austin, TX; received August 17, 2021; accepted November 22, 2021 by Editorial Board Member Shaul Mukamel

Catalysis is a method of accelerating chemical reactions that is critically important for fundamental research as well as for industrial applications. It has been recently discovered that catalytic reactions on metal nanoparticles exhibit cooperative effects. The mechanism of these observations, however, remains not well understood. In this work, we present a theoretical investigation on possible microscopic origin of cooperative communications in nanocatalysts. In our approach, the main role is played by positively charged holes on metal surfaces. A corresponding discrete-state stochastic model for the dynamics of holes is developed and explicitly solved. It is shown that the observed spatial correlation lengths are given by the average distances migrated by the holes before they disappear, while the temporal memory is determined by their lifetimes. Our theoretical approach is able to explain the universality of cooperative communications as well as the effect of external electric fields. Theoretical predictions are in agreement with experimental observations. The proposed theoretical framework quantitatively clarifies some important aspects of the microscopic mechanisms of heterogeneous catalysis.

catalysis | stochastic processes | cooperativity | diffusion

Catalysis is a set of experimental approaches that are crucial for fundamental research as well as for multiple technological applications (1, 2). In these methods, generally slow chemical reactions are significantly accelerated by adding small amounts of specific compounds, called catalysts, that are not consumed in these processes. Although catalytic phenomena have been known and intensively studied for a long time, many aspects of these complex physical–chemical processes are still not well understood (2–4). It is especially difficult to fully characterize the heterogeneous catalysis when reactants, products, and catalysts operate in distinct thermodynamic phases (5).

In recent years, nanoparticles have become important heterogeneous catalysts with multiple applications ranging from synthesis of medically important compounds to energy storage (3, 6, 7). The intrinsic heterogeneity of nanocatalysts, however, complicates understanding the mechanisms of chemical processes in these systems using ensemble bulk measurements. More microscopic information can be obtained from single-molecule experimental approaches (8–14). These studies showed that there is a wide distribution in the rates of product formations and dissociations from the nanocatalysts. In addition, there are strong temporal fluctuations in chemical reaction rates that depend on the size of the nanoparticles (15, 16). However, the most surprising observation in nanocatalysts is an apparent communication between different catalytic sites (17). Artificially similar phenomena have been observed in enzymes when catalyzed reactions occurring at different sites communicate cooperatively over distances of up to a few nanometers (18, 19). It has been argued that this is a result of allosteric processes due to local structural modifications near the active site that might propagate along the protein structures. However, in nanocatalysts, the catalytic communication definitely cannot follow the same mechanisms because these catalysts are rigid solid bodies with fixed structures. In addition, communications in nanocatalysts have been observed at much larger distances reaching hundreds of nanometers (17, 19).

To understand the microscopic mechanisms of catalytic cooperativity, single-molecule fluorescence localization microscopy has been utilized to evaluate the correlations between the subsequent time-dependent reactions occurring at different locations for single Pd- or Au-based nanocatalysts (17). In these experiments, several catalyzed reactions have been monitored in real time with high temporal and spatial resolutions on nanoparticles consisting of metal cores covered by mesoporous silica shells. By dividing the nanocatalysts into segments, the correlations between reaction times at different active sites have been measured. Surprisingly, it was found that spatially close active sites communicate with each other; the reaction that starts at one of them would have a higher probability to be followed soon by the same reaction at the neighboring active site. Interestingly, such correlations extend over distances ∼100 to 600 nm, persisting for times ∼10 to 100 s. Another striking observation was an apparent universality of intraparticle catalytic communications;

Significance

Catalysis is an experimental approach to accelerate chemical reactions. It plays a critical role in modern industries. Recent experimental studies uncovered striking observations of cooperative communications for reactions on nanocatalysts. In these experiments, it was shown that the chemical reactions observed at specific active sites might effectively stimulate the same reactions at the neighboring sites. We developed a theoretical model to investigate the microscopic mechanisms of these phenomena. Our idea is that the catalytic communication is the result of the complex dynamics of charged holes. Explicit calculations are able to quantitatively explain all experimental observations, clarifying the molecular origin of cooperative communications. The presented theoretical framework might be utilized for developing efficient catalytic systems with better control over chemical reactions.

Author contributions: S.C. and A.B.K. designed research; B.P., S.C., and A.B.K. performed research; B.P., S.C., and A.B.K. analyzed data; and B.P., S.C., and A.B.K. wrote the paper.

The authors declare no competing interest.

This article is a PNAS Direct Submission. T.D. is a guest editor invited by the Editorial Board.

This article is distributed under Creative Commons Attribution-NonCommercial-NoDerivatives License 4.0 (CC BY-NC-ND).

[1]S.C. and A.B.K. contributed equally to this work.

[2]To whom correspondence may be addressed. Email: srabanti@iiserpune.ac.in or tolya@rice.edu.

This article contains supporting information online at https://www.pnas.org/lookup/suppl/doi:10.1073/pnas.2115135119/-/DCSupplemental.

Published January 12, 2022.

Downloaded from https://www.pnas.org by FONDREN LIBRARY MS 235 on April 3, 2022 from IP address 128.42.160.175.

for a given nanocatalyst and chemical reaction, the correlation lengths and times are independent of segmentation size, laser intensity, and catalytic activity as well as the reactants concentrations. Further experiments uncovered that communications between different active sites on nanocatalysts involve positively charged messenger species, most probably charged holes on the surfaces of the nanoparticles (17). This was proven by applying the external electric fields in the direction opposing or supporting the migration flux of these particles along the catalytic nanorods.

Although experiments clearly connected the intraparticle catalytic communications with the motion of positively charged holes, many fundamental questions on the microscopic mechanisms of cooperativity in nanocatalysts remain unanswered. More specifically, why and how are catalytic communications accomplished by charged holes? What drives them between the different active sites? What is the microscopic origin of universality of the catalytic communications? How do we quantify the correlation lengths, memory times, and the effect of external electric fields?

To answer these questions, we present a theoretical framework to quantitatively describe the catalytic communications phenomena from the microscopic point of view. Our main idea is that the probability for the given active site to fire up depends on the local concentration of charged holes, and each catalyzed chemical reaction produces additional holes at this location. This creates a gradient of charged holes that drives them into the neighboring segments, temporarily increasing the local concentrations of holes there and stimulating new catalyzed reactions at closely located active sites. The memory times correspond to lifetimes of charged holes in the nanocatalysts, while the communication lengths are determined by the average distances traveled by the charged holes before they disappear. Using this hypothesis, we develop a discrete-state stochastic model of the catalytic cooperativity in nanocatalysts that can be exactly solved, providing quantitative estimates for correlation lengths, memory times, and the effect of external electric fields. Our theoretical predictions fully explain all experimental observations, and they also allow us to make experimentally testable predictions.

Methods

Let us consider a single nanocatalyst particle at which chemical reactions of only one type are taking place at active sites as illustrated in Fig. 1*A*. These processes are redox reactions that involve the transfer of charged species. Since the charged holes are important for catalytic properties of active sites (1, 4, 20–23), we hypothesize that the probability for the redox chemical reaction to fire up at the given site might be a function of the local concentration of charged holes (23, 24). In addition, it is assumed that each reaction produces new charged holes with a rate k (Fig. 1*A*). This leads to the increased local concentration of charged holes, and they start to diffuse away to other segments with lower local concentrations. This migration process is taking place with a diffusion rate u. Due to the presence of charged traps and other mechanisms (25–28), however, the lifetimes of these charged messengers are finite, and they disappear with a rate r (Fig. 1*A*). The combination of diffusion and death creates a region of the increased local density of charged holes around the active site where these messengers were initially produced. This means that there is an increased probability for the reaction to occur on the active sites in the spatially close region to the original active site. We postulate that the size of such region corresponds to the correlation length, while the mean lifetime of the charged holes determines the memory time of the catalytic communications. This is the main idea of our theoretical approach.

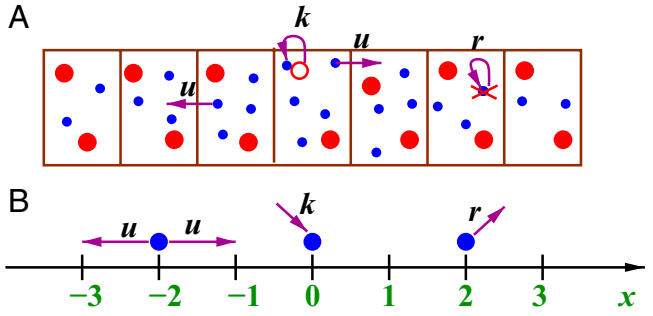

Fig. 1. (*A*) A schematic view of a catalytic nanorod with multiple active sites (red filled circles). The nanocatalyst is divided into equal-sized segments. The probability for the reaction to happen at a given site is proportional to the local concentration of charged holes (blue circles). When the reaction is taking place (at the red unfilled circle), the holes are created with a rate k. Charged holes can diffuse along the nanocatalyst with a rate u, and eventually, they will disappear with a rate r. (*B*) A corresponding discrete-state stochastic model of the catalytic cooperativity. Lattice sites $x = 0, \pm 1, \pm 2, \ldots$ label different segments of the nanorod. The charged hole appears first at the segment $x = 0$ at time $t = 0$. It diffuses along the lattice with the rate u until it dies with rate r.

To quantify our theoretical arguments, we introduce a discrete-state stochastic model as presented in Fig. 1*B*. Since most investigated catalytic particles were nanorods, we adopt a one-dimensional description. The lattice describes the nanorod divided into segments, and the distance between neighboring lattice segments, l, corresponds to the size of the segment $\sim$100 nm in experimental settings (17). Note that there might be multiple active sites in each segment. To simplify calculations, we also adopt a single-particle view of the dynamics in the system. At time $t = 0$, the charged hole appears at the given site of the segment n that we choose as $x = 0$ in our lattice description with the rate k (Fig. 1*B*). This hole can diffuse along the lattice with the diffusion rate u, and it eventually disappears with the rate r (Fig. 1*B*). We assume that the produced hole can explore a large part of the nanorod before the production of another hole. In addition, the nanocatalysts are considered as very long ($|x| \to \infty$ in Fig. 1*B*), although the analysis can also be extended for the finite-sized nanorods, as shown in detail in *SI Appendix*. The main goal of our calculations here is to show that there is a region of increased local concentration of charged holes around the active site where they were originally created after the chemical reaction fired up.

Let us define $P_n(t)$ $(n = 0, \pm 1, \pm 2, \ldots)$ as the probability density function of finding the messenger at the segment n at time t if at $t = 0$, it was created at the segment $n = 0$. This function is proportional to the local concentration of charged holes. In addition, we might have a situation when the charged hole is not produced yet, while the earlier produced messenger already died. It is described by the probability density function $P_{off}(t)$. The temporal evolution of these probability density functions is governed by a set of master equations:

$$\begin{aligned}
\frac{dP_n(t)}{dt} &= uP_{n-1}(t) + uP_{n+1}(t) - (2u + r)P_n(t);\\
\frac{dP_0(t)}{dt} &= uP_{-1}(t) + uP_1(t) + kP_{off}(t) - (2u + r)P_0(t);\\
\frac{dP_{off}(t)}{dt} &= r\sum_{n=-\infty}^{+\infty} P_n(t) - kP_{off}(t). \qquad [1]
\end{aligned}$$

In addition, we have a normalization condition:

$$P_{off}(t) + \sum_{n=-\infty}^{+\infty} P_n(t) = 1. \qquad [2]$$

Downloaded from https://www.pnas.org by FONDREN LIBRARY MS 235 on April 3, 2022 from IP address 128.42.160.175.

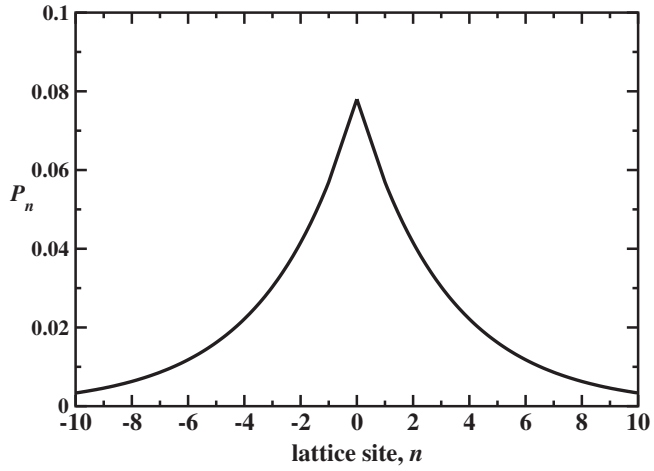

Fig. 2. Stationary distribution of probabilities of finding the charged holes particles near the position where they were produced in the chemical reaction on site 0. Parameters used in calculations are $u = 10\ s^{-1}$ and $r = k = 1\ s^{-1}$.

Assuming that the stationary distribution of finding the charged hole at the lattice sites around the place where it was produced ($n = 0$ in Fig. 1*B*) can be achieved fast, one can calculate these steady-state probability density functions, as shown in detail in *SI Appendix*:

$$P_{off} = \frac{r}{r+k} = \frac{a}{a+b}; \quad [3]$$

$$P_n(t) = By^{|n|}, \quad n = \pm 1, \pm 2, \ldots; \quad [4]$$

$$P_0 = \frac{2By + \frac{ab}{a+b}}{(a+2)}, \quad [5]$$

where $a \equiv r/u$ and $b \equiv k/u$, and other parameters are given by

$$y = 1 + a/2 - \sqrt{a^2/4 + a} \quad [6]$$

and

$$B = \frac{b(1-y)}{y(a+b)(3+a-y)}. \quad [7]$$

The calculated stationary distribution of probabilities to find the charged hole around the place where it was initially produced is presented in Fig. 2. One can see that there is an increased probability to find the messenger at the same place ($n = 0$), and the distribution exhibits the exponential decay as the distance from the origin increases. This defines a specific length scale λ (in units of the segment size l) associated with the decay:

$$\lambda = -\frac{1}{\ln y}. \quad [8]$$

The physical meaning of this length is that it corresponds to the size of the region with the increased local concentration of charged holes due to the initial production at the active site at $n = 0$. This allows us to associate it with the correlation length of catalytic communications because as we postulated, in the region $[-\lambda, \lambda]$ there will be an increased probability of firing up the chemical reaction at another active site.

If the lifetime of the charged hole is very short ($r \gg 1$, $a \gg 1$), we obtain $y \simeq 2/a$, and the correlation length of the catalytic communication will be very short, $\lambda \sim 1/\ln a$. In this case, the charged holes cannot create a significant region with the increased local density of messengers, and thus, weak or no catalytic communication is expected. In a more realistic scenario, the charged holes are quite stable ($r \to 0$, $a \to 0$), and we have $y \simeq 1 - \sqrt{a}$ with the correlation length being equal to $\lambda \simeq 1/\sqrt{a}$. This means that the region of cooperativity in the catalysis on nanorods is solely determined by the balance between the diffusion and death rates of the messenger particles ($a = r/u$). Note that it does not depend on the charged hole production rate k.

Results

Catalytic Communications in Metallic Nanorods. Now we can apply our theoretical approach for clarifying the microscopic mechanisms that lead to the catalytic communications phenomena observed recently on metal nanocatalysts (17). In these experiments, various redox chemical reactions have been catalyzed on single Pd and Au nanorods. More specifically, the photo-induced disproportionation of resazurin (Rz) to generate fluorescent resorufin on Pd nanorods, the oxidative deacetylation of the amplex red (AR) into the fluorescent resorufin by H_2O_2, and the reductive deoxygenation of Rz to fluorescent resorufin by NH_2OH on Au nanorods have been comprehensively analyzed (17).

We associate the measured memory time τ as the inverse death rate for the charged holes, $r = 1/\tau$. For measuring the correlations in reaction times, the nanorods were divided into segments of length $l \simeq 100$ nm, and the diffusion constants D of the messengers were also measured in these experiments (17). This allows us to evaluate the effective migration rate in our discrete-state stochastic model as $u = 2D/l^2$. Finally, the correlation lengths are calculated explicitly using Eq. **8** with $y \simeq 1 - \sqrt{a}$. The results of our theoretical calculations for Pd and Au single nanocatalysts and the comparison with experimental measurements are presented in Table 1. An excellent agreement between theoretical predictions and experimental values is observed for all investigated systems, strongly supporting our theoretical approach.

In experimental studies, the correlation lengths and memory times in the catalytic communications were specifically obtained by analyzing a Pearson's cross-correlation coefficient between chemical reaction times for different events on different segments (17). This parameter provides a quantitative measure of how the catalyzed chemical reactions at different sites and at different times are correlated with each other. A positive value of the Pearson coefficient was attributed to a sign of the existence of cooperative communications in the nanocatalysts. Our discrete-state stochastic model is also convenient for calculating the Pearson's cross-correlation coefficient, providing an important test on the validity of the proposed theoretical approach. To make the comparison between experiments and theory more realistic,

Table 1. Comparison of experimentally determined and theoretically calculated correlation lengths in the catalytic communication

	Pd nanorods (Rz disproportionation)	Au nanorods (AR deacetylation)	Au nanorods (Rz deoxygenation)
Lifetimes, τ (s), experimental	27.5 ± 2.4	128 ± 32	168 ± 36
Diffusion constants, D ($10^{-15} m^2\ s^{-1}$), experimental	0.92 ± 0.08	1.1 ± 0.4	1.2 ± 0.4
Correlation lengths, experimental (nm)	225 ± 20	516 ± 160	624 ± 180
Correlation lengths, theoretical (nm)	225 ± 20	531 ± 164	635 ± 175

Data are taken from ref. 17. The theoretical correlation lengths are calculated using Eq. **8**.

Downloaded from https://www.pnas.org by FONDREN LIBRARY MS 235 on April 3, 2022 from IP address 128.42.160.175.

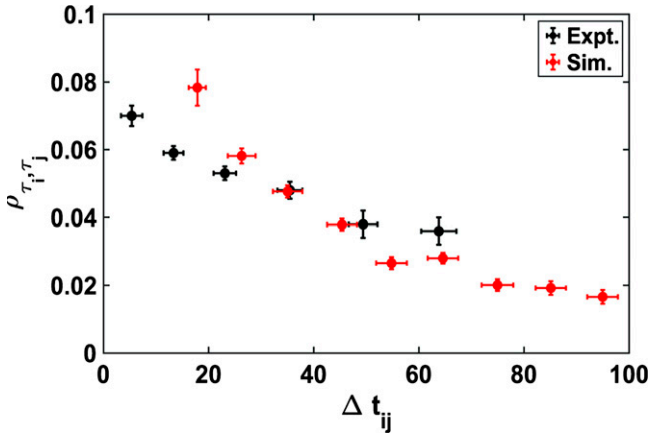

Fig. 3. Experimental (Expt.; black symbols; from ref. 17) and the simulated (Sim.; red symbols) Pearson's cross-correlation coefficients vs. average time separation ($\triangle t_{ij}$) of temporally subsequent reactions at two different segments on the same Pd nanorod. Parameters used in theoretical calculations are $r = 0.036\ s^{-1}$, $u = 0.184\ s^{-1}$, $k = 0.0145\ s^{-1}$, and $n = 700$. Details of the simulation procedure are given in *SI Appendix*.

we utilized Monte Carlo computer simulations of the discrete-state stochastic model as explained in *SI Appendix*. The results obtained from simulations are presented in Fig. 3. One can see that the calculated correlation agrees well with experimentally obtained values. Importantly, our analysis produces the same range of amplitudes for the Pearson's coefficient, and the decay is also clearly observed. This gives the additional support to our theoretical model.

Experimental results exhibit relatively low amplitudes of correlations. Our theoretical approach can explain these observations by noting that the experimentally observed migration rates are relatively slow (we estimate from experimental data that $u \simeq 0.184\ s^{-1}$ for Pd nanoparticles and $u \simeq 0.23\ s^{-1}$ for Au nanoparticles), and the correlations are measured for active sites located at different segments at relatively long distances of ~100 nm. We propose then that the low amplitude of the reported correlations might be the result of the following factors: large distances between the active sites where the correlations are measured, low rates of the charged holes diffusion that lead to the limited influx to other active sites, and possibly, large densities of already present charged holes that are only weakly modified by the incoming migration fluxes of the holes. However, importantly, these arguments also suggest additional ways of testing the proposed theoretical model. We predict that the amplitude of correlations will increase if the correlations are to be measured for the active sites that are closer to each other and for increasing the flux of incoming charged holes to new active sites (via accelerating the diffusion rates or making more holes during the catalyzed chemical reactions).

The Effect of External Electric Field. To probe the origin of catalytic communications in single nanocatalysts, the correlations have been also measured under conditions when the external voltage has been applied (17). It was found that the communication distance in the downfield direction increased while the same distance in the opposite direction decreased. In addition, these correlation lengths showed a cosinusoidal modulation as a function of the angle between the field and the axis of the nanorod. Furthermore, these distances exhibited a linear scaling with the increased applied voltage, at least for the strengths of external fields utilized in these experiments. These observations allowed researchers to conclude that the catalytic cooperativity is due to positively charged messenger species (17). Since several quantitative results on the effect of external fields have been obtained, it is important to test if our theoretical model can explain these observations.

In our approach, under an external electric field, the effective diffusion rate of the charged holes to move between neighboring segments will be different depending on the angle between the nanorod and the applied voltage,

$$u^{\pm} = u \exp\left[\pm \frac{m\Delta\varepsilon \cos\phi}{k_B T}\right], \qquad [9]$$

where ϕ is the angle, m is the number of holes that pass the border between segments per unit time, and $\Delta\varepsilon$ is the energy needed to move one charged messenger from one segment to the next one. It is given by

$$\Delta\varepsilon = \frac{q|V|l}{d}, \qquad [10]$$

where q is the charge of a single hole, $|V|$ is the strength of the applied voltage, d is the distance between electrodes in the external voltage experiments, and l is the size of the segment. Thus, in the absence of the external field, the charged holes exhibit an unbiased diffusion motion, while the introduction of the applied voltage changes the character of the motion to be the biased diffusion. This is the main effect of the external field according to our theoretical picture.

On average, charged holes have a lifetime $\tau = 1/r$ before they disappear. Then, the increase in the communication length in the direction favored by the external field in comparison with the opposite direction (in units of the segment length l) is given by

$$\frac{\Delta x_{0,EF}}{l} = (u^{+} - u^{-})\tau \simeq \frac{2u}{r}\ \frac{m\Delta\varepsilon\cos\phi}{k_B T}. \qquad [11]$$

The last expression is an approximation because at typical experimental conditions $|V| \sim 1$ V, $l = 100$ nm, and $d \simeq 1$ to 10 mm, it yields a very small energy cost of moving the single charged hole between the segments, $\Delta\varepsilon \sim 0.001$ to $0.01\ k_B T$. In addition, the parameter m (number of charged holes passing the border between two neighboring segments per unit time) is also expected to be not very large. This allows for the expansion of the exponent in Eq. **9**, yielding the result in Eq. **11**.

Our main quantitative result given in Eq. **11** has three important predictions. First, it argues that the catalytic communication distances in the external electric field, $x_{0,EF} = x_0 + \Delta x_{0,EF}$ with x_0 being the voltage-free correlation length, will exhibit a cosine dependence in the orientation angle relative to the electric field direction. It is explicitly illustrated in Fig. 4, and excellent agreement with experimental observations is found. Our theoretical picture naturally explains the cosine dependence, suggesting that this is the consequence of the relatively weak external voltages. For stronger fields or large fluxes between segments (larger m), we predict that the behavior would have a stronger exponential dependence on the cosine of the orientation angle (Eq. **9**). This is a prediction that can be tested experimentally.

The second conclusion from Eq. **11** is that the change in the communication length, $\Delta x_{0,EF}$, depends linearly on the applied voltage as suggested by Eq. **10**. In Fig. 5, we compare theoretical predictions with experimental observations for different voltages. Again, a linear trend in the dependence of $\Delta x_{0,EF}$ as a function of $|V|$ is clearly observed. These findings give additional support to our theoretical model, emphasizing the important role of charged holes and their dynamics.

A third conclusion from Eq. **11** is that under the external field, the correlation length depends linearly on the diffusion rate and the lifetime, in contrast to the field-free case when the correlation length depends on a square root of the diffusion rate and the lifetime of the charged holes (our results are given above). It is important also to note that our theoretical model predicts that the memory times are independent of the external field because

Downloaded from https://www.pnas.org by FONDREN LIBRARY MS 235 on April 3, 2022 from IP address 128.42.160.175.

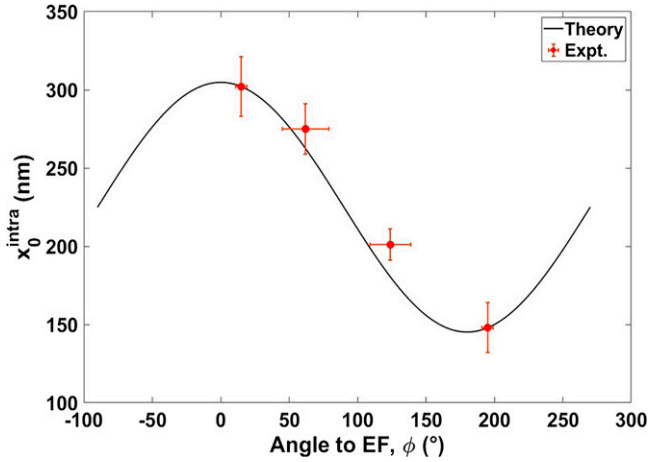

Fig. 4. Dependence of the catalytic communication distance for temporally subsequent reactions at two different segments as a function of the orientation angle ϕ at the given voltage from the discrete-state stochastic model. Red symbols with error bars are the experimental data (Expt.) on Pd nanorods catalyzing the photo-induced disproportionation of the compound Rz as described in ref. 17. Parameters used for calculations are $r = 0.0364\ s^{-1}$, $u = 0.184\ s^{-1}$, $q = 1.6 \times 10^{-19}$ C, $l = 100$ nm, $d = 1$ mm, $V = 1.2$ V, and $m = 17$.

the death rate does not depend on the applied voltage, again in agreement with experimental observations (17).

An important parameter in the transport of charged messengers is m, which gives the flux of the charged holes crossing from one segment to another per unit time. By comparing our theoretical predictions with experimental observations, we can explicitly determine this quantity for different systems. It can be shown that $m \simeq 17.1$ for Rz disproportionation on Pd nanorods, $m \simeq 4.6$ for AR deacetylation on Au nanorods, and $m \simeq 3.0$ for Rz deoxygenation on Au nanorods. In all these situations, these numbers are not large so that the expansion of the exponential term in Eq. **9** is justified, producing the cosine dependence of the modulation of the correlation length on the orientation angle. It is also reasonable that the values of m for Au nanorods are similar for different reactions ($m \simeq 4.6$ and $m \simeq 3$). It will be interesting to compare these theoretical predictions with real experimental measurements of these quantities.

It is expected that the number of charged holes on the surface of the catalytic nanoparticle is probably quite large, and it is surprising that our analysis identifies only a few holes migrating between the segments per unit time. There are two possible reasons for such observations. First, it is possible that experiments could not determine all migrating holes due to the limitations in their detecting setups. Second, if the number of created holes after every catalyzed event is not large in comparison with the already existing number of charged holes at this location, then the gradient that drives the diffusion of holes will not be significant. We believe that the second reason is more probable because it is also supported by the low amplitudes of the correlations reported from the experiments (Fig. 3).

Discussion

We presented a comprehensive theoretical approach to investigate the microscopic origin of intraparticle catalytic communications in metallic nanocatalysts. In our method, it is assumed that the properties of positively charged holes play a main role in correlating chemical reactions on different active sites of single catalytic nanoparticles. Our idea is that these reactions depend on the local concentration of charged holes, and these reactions also produce them, creating the local gradients that lead to the diffusive fluxes of these particles to different parts of the nanocatalyst. Because the probability of the reaction to occur at the given active site depends on the local concentration of the charged holes, the temporary increased concentration of charged holes stimulates the reactions in the spatially close region. Since the charged holes eventually disappear, the balance between the diffusion and the death processes defines the effective length scale of the catalytic communication, while the charged holes lifetimes determine the memory times of the catalytic cooperativity.

Using these theoretical arguments, we developed a fully quantitative discrete-state stochastic model that explicitly evaluates the lifetimes of the charged holes and the correlation lengths of the catalytic communications. It was also shown that our theoretical method could quantitatively explain the effect of external applied voltages on the catalytic communication. In our theoretical picture, the external field modifies differently the effective diffusive rates in the field direction and against the field. We found that our theoretical predictions are in excellent agreement with all available experimental observations of catalytic communications in metal nanocatalysts.

The essence of our theoretical idea is that the nanocatalysts function via a mechanisms that is similar to branched chemical reactions (29). These processes have been studied in macroscopic catalysts, and they can give rise to various interesting phenomena, such as traveling waves and other nonlinear effects (30). It will be interesting to probe from this angle the catalytic communications in nanocatalysts.

While our theoretical approach can quantitatively describe all features of the catalytic communications, its most important contribution is the ability to explain the universality of such nanocatalyst cooperativity effects from the microscopic point of view (17). It was found experimentally that the intraparticle catalytic cooperativity is independent of the experimental time resolutions, the segmentation size, the laser intensity, nanorod's catalytic activity, details of the fluorescence measurements, and the concentrations of reactants in catalyzed chemical reactions. All these properties of the systems are not influenced by the diffusion and the death rates of the charged holes that specify the microscopic picture of the catalytic communications. Thus, the correlations can be affected only by changing the dynamics and lifetimes of the charged messengers. For example, using

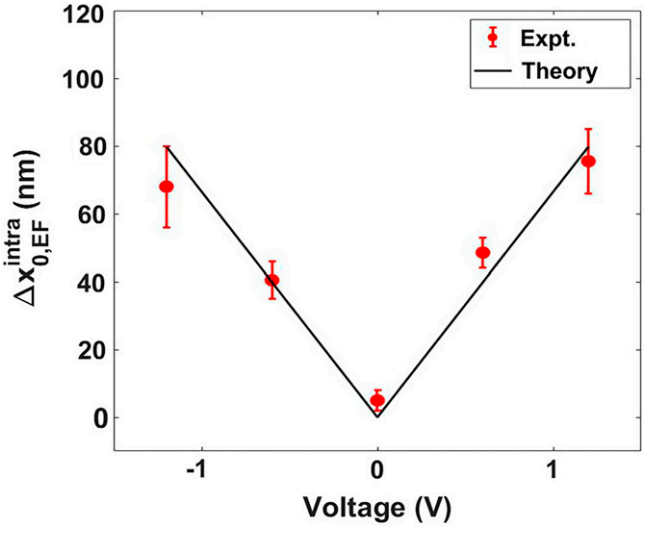

Fig. 5. Dependence of the amplitude of the catalytic communication length variation as a function of the applied voltage calculated using our theoretical model (solid black line). Red symbols with error bars correspond to the experimental data (Expt.) on Pd nanorods as discussed in ref. 17. Parameters used for calculations are $r = 0.03636\ s^{-1}$, $u = 0.184\ s^{-1}$, $q = 1.6 \times 10^{-19}$ C, $l = 100$ nm, $m = 17.1$, and $d = 1$ mm.

Downloaded from https://www.pnas.org by FONDREN LIBRARY MS 235 on April 3, 2022 from IP address 128.42.160.175.

our theoretical method, one can argue how the increase in the temperature might influence the catalytic communications. Since the death rate will increase with T, this would decrease the memory time. However, the effect on the correlation length would depend on what rate, diffusion or death, grows faster with the temperature. If the diffusion rate increases quicker, then we expect to have larger communication distances with the temperature increase. The opposite effect is expected when the death rate of the charged holes changes faster than the diffusion rate. It will be interesting to test these theoretical predictions, as well as others discussed in this work, in experimental studies.

The proposed microscopic picture of catalytic communications raises a question on how to improve the efficiency of heterogeneous catalytic processes. There are significant efforts in developing new artificial enzyme mimics of catalysts with controlled chemical properties, and metal nanocatalysts with cooperative correlations might be a good candidate for such developments (31). Several specific suggestions to improve the catalytic efficiency can be made based on our theoretical arguments. It seems reasonable that the most efficient strategy would be to utilize nanocatalysts where the distances between the active sites are shorter than the correlation lengths. This would ensure the increased activity in all the nanocatalyst system. One could also tune the catalytic efficiency by varying the density of charged holes and density of traps that kill them (32). There are multiple experimental techniques to affect the concentrations of charged holes, including various photochemical and electrochemical methods. Furthermore, one could suggest that the nanocatalysts with more rough surfaces would have a larger amount of active sites, leading to more efficient catalysts. It is also interesting to note that our ideas on importance of charged holes in catalytic processes are related to recent proposals on the role of charged holes in organic electrosynthesis and photochemical water oxidation (33, 34).

It is also important to discuss the limitations of our approach. The detailed microscopic mechanisms of how charged holes specifically stimulate the reaction on the active sites and how the additional charged holes are produced after such reactions are not discussed in our model (4). This is because more detailed quantum-mechanical and electronic structure information is needed to clarify these issues, and they are beyond of the scope of our study. In addition, these details probably will not affect the dynamics and lifetimes of charged messengers, and thus, they will not influence the cooperativity observed in the metal nanocatalysts. However, we still might present the following semiphenomenological arguments. The experimentally investigated processes are redox chemical reactions that have been carried out on nanocatalyst particles that consist of metal cores covered by silica shells (17). It was argued that the metal surfaces are oxidized, allowing for the existence of localized charged holes on the surfaces (instead of delocalized holes in bulk metals). Considering that all the active sites are present on the surface only, we might assume that a high local concentration of charged holes is associated with the presence of active sites. This is because the incoming substrates might donate electrons to the nearby holes, leading to effective interactions that allow the catalyzed processes to occur. Moving the charges to the product molecules can also create more charged holes at this location. Of course, these arguments are quite speculative, and most probably, more complex processes are occurring in these systems. However, at the minimum, our theoretical method provides an effective quasiclassical mesoscopic description of catalytic communications that, due to its quantitative nature, might still provide some useful insights.

Our theoretical model also considers an effectively one-dimensional picture, while real catalysts are three-dimensional objects. In addition, it is assumed that the stationary dynamics are very quickly reached in the system, but this should be tested more carefully. Furthermore, the diffusion and death rates of the charged holes are assumed to be constant in time and uniform along the nanocatalyst, while it is more realistic to expect these transition rates to be spatially and temporary heterogeneous. It remains unclear how this heterogeneity would affect the catalytic communications effect. However, despite these limitations, our theoretical method provides a physically consistent microscopic picture that also allows for a comprehensive quantitative description of the correlations in chemical reactions catalyzed on single nanoparticles. Thus, our theoretical method clarifies important aspects of the fundamental mechanisms of the complex processes that are taking place during the heterogeneous catalysis.

Data Availability. All study data are included in the article and/or *SI Appendix*.

ACKNOWLEDGMENTS. B.P. acknowledges the Prime Minister's Research Fellowship and the Indian Institue of Science Education and Research (IISER) Pune–IDEAS Scholarship for a fellowship. S.C. acknowledges IISER Pune for facilities and SERB, India (CRG/2019/000 515) for funding. A.B.K. acknowledges support from Welch Foundation Grant C-1559, from NSF Grants CHE-1953453 and MCB-1941106, and from the Center for Theoretical Biological Physics sponsored by NSF Grant PHY-2019745.

1. G. A. Somorjai, Y. Li, *Introduction to Surface Chemistry and Catalysis* (John Wiley & Sons, 2010).
2. J. R. Ross, *Heterogeneous Catalysis: Fundamentals and Applications* (Elsevier, 2011).
3. D. Astruc, Introduction: Nanoparticles in catalysis. *Chem. Rev.* **120**, 461–463 (2020).
4. Z. Zhang, B. Zandkarimi, A. N. Alexandrova, Ensembles of metastable states govern heterogeneous catalysis on dynamic interfaces. *Acc. Chem. Res.* **53**, 447–458 (2020).
5. I. Fechete, Y. Wang, J. C. Védrine, The past, present and future of heterogeneous catalysis. *Catal. Today* **189**, 2–27 (2012).
6. A. Corma, H. Garcia, Supported gold nanoparticles as catalysts for organic reactions. *Chem. Soc. Rev.* **37**, 2096–2126 (2008).
7. H. M. T. Galvis *et al.*, Supported iron nanoparticles as catalysts for sustainable production of lower olefins. *Science* **335**, 835–838 (2012).
8. W. E. Moerner, Single molecules observed by near-field scanning optical microscopy. *Rev. Sci. Instrum.* **74**, 3597–3619 (2003).
9. E. Betzig, R. J. Chichester, Single molecules observed by near-field scanning optical microscopy. *Science* **262**, 1422–1425 (1993).
10. P. Chen *et al.*, Spatiotemporal catalytic dynamics within single nanocatalysts revealed by single-molecule microscopy. *Chem. Soc. Rev.* **43**, 1107–1117 (2014).
11. W. Xu, J. S. Kong, Y. T. Yeh, P. Chen, Single-molecule nanocatalysis reveals heterogeneous reaction pathways and catalytic dynamics. *Nat. Mater.* **7**, 992–996 (2008).
12. W. Xu, J. S. Kong, P. Chen, Probing the catalytic activity and heterogeneity of Au-nanoparticles at the single-molecule level. *Phys. Chem. Chem. Phys.* **11**, 2767–2778 (2009).
13. T. Chen, Y. Zhang, W. Xu, Single-molecule nanocatalysis reveals catalytic activation energy of single nanocatalysts. *J. Am. Chem. Soc.* **138**, 12414–12421 (2016).
14. J. E. Maris, D. Fu, F. Meirer, B. M. Weckhuysen, Single-molecule observation of diffusion and catalysis in nanoporous solids. *Adsorption* **27**, 423–452 (2021).
15. C. Burda, X. Chen, R. Narayanan, M. A. El-Sayed, Chemistry and properties of nanocrystals of different shapes. *Chem. Rev.* **105**, 1025–1102 (2005).
16. X. Zhou, W. Xu, G. Liu, D. Panda, P. Chen, Size-dependent catalytic activity and dynamics of gold nanoparticles at the single-molecule level. *J. Am. Chem. Soc.* **132**, 138–146 (2010).
17. N. Zou *et al.*, Cooperative communication within and between single nanocatalysts. *Nat. Chem.* **10**, 607–614 (2018).
18. Q. Cui, M. Karplus, Allostery and cooperativity revisited. *Protein Sci.* **17**, 1295–1307 (2008).
19. R. Ye, X. Mao, X. Sun, P. Chen, Analogy between enzyme and nanoparticle catalysis: A single-molecule perspective. *ACS Catal.* **9**, 1985–1992 (2019).
20. W. Sapp, R. Koodali, D. Kilin, Charge transfer mechanism in titanium-doped microporous silica for photocatalytic water-splitting applications. *Catalysts* **6**, 34 (2016).
21. L. Zhang, H. H. Mohamed, R. Dillert, D. Bahnemann, Kinetics and mechanisms of charge transfer processes in photocatalytic systems: A review. *J. Photochem. Photobiol. C* **13**, 263–276 (2012).
22. M. H. Jang *et al.*, Synergetic effect on catalytic activity and charge transfer in Pt-Pd bimetallic model catalysts prepared by atomic layer deposition. *J. Chem. Phys.* **152**, 024710 (2020).
23. O. R. Luca, J. L. Gustafson, S. M. Maddox, A. Q. Fenwick, D. C. Smith, Catalysis by electrons and holes: Formal potential scales and preparative organic electrochemistry. *Org. Chem. Front.* **2**, 823–848 (2015).
24. A. Studer, D. P. Curran, The electron is a catalyst. *Nat. Chem.* **6**, 765–773 (2014).
25. Z. Bian, T. Tachikawa, W. Kim, W. Choi, T. Majima, Superior electron transport and photocatalytic abilities of metal-nanoparticle-loaded tio2 superstructures. *Chem. Soc. Rev.* **116**, 25444–25453 (2012).
26. L. Chernyak, A. Osinsky, V. Fuflyigin, E. Schubert, Electron beam-induced increase of electron diffusion length in p-type gan and algan/gan superlattices. *Appl. Phys. Lett.* **77**, 875–877 (2000).

Downloaded from https://www.pnas.org by FONDREN LIBRARY MS 235 on April 3, 2022 from IP address 128.42.160.175.

27. J. Gonzalez-Vazquez, J. A. Anta, J. Bisquert, Determination of the electron diffusion length in dye-sensitized solar cells by random walk simulation: Compensation effects and voltage dependence. *J. Phys. Chem. C* **114**, 8552–8558 (2010).
28. J. K. Utterback *et al.*, Observation of trapped-hole diffusion on the surfaces of CdS nanorods. *Nat. Chem.* **8**, 1061–1066 (2016).
29. P. L. Houston, *Chemical Kinetics and Reaction Dynamics* (Courier Corporation, 2012).
30. M. Feinberg, D. Terman, Traveling composition waves on isothermal catalyst surfaces. *Arch. Ration. Mech. Anal.* **116**, 35–69 (1991).
31. Y. Huang, J. Ren, X. Qu, Nanozymes: Classification, catalytic mechanisms, activity regulation, and applications. *Chem. Rev.* **119**, 4357–4412 (2019).
32. J. Rozen *et al.*, Increase in oxide hole trap density associated with nitrogen incorporation at the sio 2/sic interface. *J. Appl. Phys.* **103**, 124513 (2008).
33. R. Francke, R. D. Little, Electrons and holes as catalysts in organic electrosynthesis. *ChemElectroChem* **6**, 4373–4382 (2019).
34. Y. Zhang *et al.*, Modulating multi-hole reaction pathways for photoelectrochemical water oxidation on gold nanocatalysts. *Energy Environ. Sci.* **13**, 1501–1508 (2020).

Downloaded from https://www.pnas.org by FONDREN LIBRARY MS 235 on April 3, 2022 from IP address 128.42.160.175.